Fast far-sidelobe modeling for centimeter to sub-millimeter astrophysical observations

Oliver Jeong, a,b,1 Jacques Delabrouille, a,b,1 and Michel Piatc,a,b

^aCNRS-UCB International Research Laboratory, Centre Pierre Binétruy, IRL 2007, CPB-IN2P3, Berkeley, CA 94720, USA

^bLawrence Berkeley National Laboratory,

1 Cyclotron Road, Berkeley, CA 94720, USA

 $^c {\rm Universit\acute{e}}$ Paris Cité, CNRS, Astroparticule et Cosmologie, F-75013 Paris, France

E-mail: objeong@lbl.gov, delabrouille@apc.in2p3.fr, piat@apc.in2p3.fr

Abstract. Next-generation centimeter to sub-millimeter telescopes require exquisite control over instrumental far-sidelobe response to accurately measure faint signals like the Cosmic Microwave Background B modes. Because existing electromagnetic modeling methods are computationally expensive, we developed a novel, diffraction-based beam modeling method for rapid and low-cost calculations. We applied this methodology to model the BICEP3 far-sidelobes and found good qualitative agreement with in situ beam measurements. Using this validated simulated beam, we calculated the sidelobe temperature pickup for a specific observation scenario: scanning near the slopes of Cerro Toco in the Atacama Desert. This rapid, predictive framework is most valuable as a tool for optimizing instrument baffling and identifying efficient scan strategies during the conceptual design phase.

¹Corresponding author.

\mathbf{C}	ontents		
1	1 Introduction		
2	2 Problem of stray radiation		
3	Diffraction-based method of modeling far sidelobe response 3.1 Electromagnetic principles of diffraction	3	
4	3.2 Review of the method Results	3	
	 4.1 Simulated sidelobe maps 4.2 Application to assess sidelobe pickup in Atacama Desert 	4 7	

7

1 Introduction

Conclusion

Since its discovery by Penzias and Wilson, observations of the cosmic microwave background (CMB) have been instrumental in establishing the concordance model of cosmology. Over the past five decades, CMB experiments have measured its anisotropies with remarkable precision, significantly advancing our understanding of the composition and evolution of the Universe. Current and forthcoming experiments are designed to search for the degree-scale parity-odd B-mode polarization pattern of the CMB — a signature imprint of primordial gravitational waves generated during cosmic inflation. The observation of such a signal would provide compelling evidence for inflation, the theorized period of exponential expansion in the early Universe, and shed light on physics at the Grand Unified Theory scales. However, this primordial B-mode signal is expected to be extremely faint and remains undetected by current CMB experiments.

As next-generation CMB experiments approach unprecedented sensitivity levels, we must demonstrate exquisite knowledge and control of instrumental systematics of its small aperture telescopes (SAT) to detect primordial B modes. Stray radiation pick-up through the imperfectly known sidelobes of the optical response of the instrument, also called the beam, is a significant source of instrumental systematic uncertainty in the observations. Far sidelobe response is particularly difficult to characterize both through modeling and measurement and thus remains an active area of investigation. This challenge is especially pronounced for ground-based experiments, where contamination from ground pickup through far sidelobes is a major concern. Modeling diffraction requires a detailed electromagnetic model, which is computationally expensive and impractical for large optical systems. In this paper, we present a simplified approach to modeling diffraction in optical systems relevant to small aperture CMB telescopes.

The paper is organized as follows. In Section 2, we briefly review the problem of far sidelobes for ground-based millimeter telescopes. In Section 3, we introduce the diffraction-based method of modeling beams for these telescopes. In Section 4, we use this method to simulate the far sidelobe response of a BICEP3-like telescope and compare the results with in situ beam measurements. Then this framework is extended to calculate the expected power

pickup of the far sidelobe response of a BICEP3-like telescope observing on the slopes of Cerro Toco in the Atacama Desert of Chile. We conclude with Section 5.

2 Problem of stray radiation

Ground-based millimeter-wave telescopes, such as those used for detecting faint signals like the CMB B modes or fluctuations of atomic and molecular emission lines, face a critical challenge: their detectors are highly susceptible to spurious signals from unwanted sources. The most concerning systematics include stray radiation from the ground and bright celestial objects like the Sun. To mitigate excessive contamination, observations must be constrained to ranges of allowed azimuth and elevations, ensuring that the brightest sources of stray radiation are kept far from the telescope's line of sight. This strategy significantly degrades the observing efficiency and can still lead to reduced data quality from residual contamination, making a precise understanding of the far-sidelobe response essential for proper shielding and baffling design.

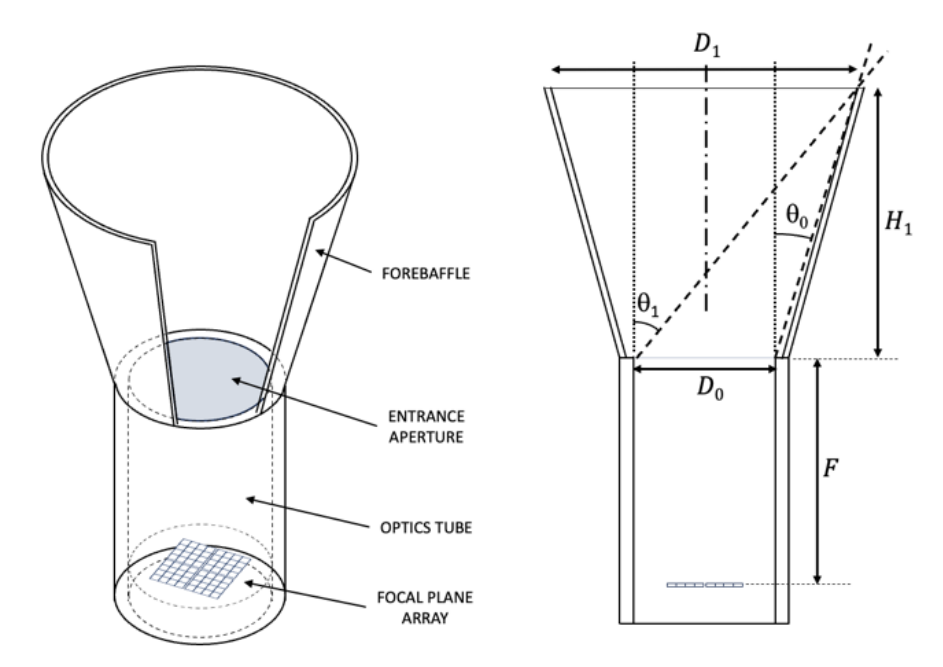


Figure 1. Diagram of optical configuration used in this study with key parameters labeled, as listed in Table 1.

As shown in Figure 1, a typical CMB *B*-mode detection telescope features a main optics tube containing cold optics and a focal plane of highly sensitive detectors. To block stray radiation, these instruments incorporate several levels of shielding: a fixed ground shield is deployed first, and an additional co-moving forebaffle is placed atop the optics tube. These forebaffles are usually conical or cylindrical tubes whose inner surfaces are engineered for maximum absorption across all incident angles.

The detectors are sensitive to any source of incoming radiation, meaning that their data streams register the integral of fluctuations from various forms of stray radiation. These contamination sources fall into four main categories: 1) Specular reflection of off-axis rays causing "ghost beams" or strong sidelobes; 2) Scattering of microwave radiation by surfaces optically coupled to the detectors, such as the vacuum window or entrance aperture; 3) Diffraction of

microwave radiation by the rims of the internal shields and baffles; and 4) Thermal emission from the instrument itself, often due to absorbed sunlight being re-emitted. All these effects become problematic when strong radiation sources, like mountains or the Sun, illuminate the instrument's interior. Diffraction is particularly unavoidable and often represents the dominant sources of off-axis radiation pickup in CMB telescopes. While ray-tracing or physical optics software can be used to calculate the sidelobe response, accurate modeling requires a precise and computationally expensive definition of the entire instrument geometry, which is only feasible up to a certain level of approximation. The reader is encouraged to refer to [1] for more detailed review of sources of stray light.

3 Diffraction-based method of modeling far sidelobe response

3.1 Electromagnetic principles of diffraction

In this paper, we use the geometric theory of diffraction to model the propagation of light between the sky and the focal-plane of the telescope. Geometric optics is the simplest model of light propagation, in which rays travel in straight lines until refracted or reflected as described by Snell's law and Fresnel equations, respectively. When the light encounters an aperture or object, it deviates from straight-line propagation and diffracts. The Huygens-Fresnel principle explains this deviation by positing that every point on a wavefront acts as a source of secondary spherical wavelets, which subsequently mutually interfere and their superposition forming a new wavefront. When a wavefront encounters an aperture, only the portion of the wavefront within the transparent opening acts as a source of secondary wavelets. These wavelets then collectively form a new wavefront that bends, or diffracts, around the edges of the aperture. This is mathematically formalized by the Rayleigh-Sommerfeld diffraction integral,

$$E(x,y,z) = \frac{1}{i\lambda} \iint_{-\infty}^{+\infty} E(x',y',0) \frac{e^{ikr}}{r} \frac{z}{r} \left(1 + \frac{i}{kr}\right) dx' dy'$$
(3.1)

describing the propagation of the electric field in the aperture E(x', y', 0) to (x, y, z) where $r = \sqrt{(x - x')^2 + (y - y')^2 + z^2}$ and k is the wavenumber $2\pi/\lambda$. We can further approximate the propagation of light to the far-field regime with the Fraunhofer diffraction equation,

$$E(x,y,z) = \frac{e^{ik\left(z + \frac{x^2 + y^2}{2z}\right)}}{i\lambda z} \iint_{\text{A perture}} E\left(x', y', 0\right) e^{-i\frac{k}{z}(xx' + yy')} dx' dy'. \tag{3.2}$$

For an arbitrary electric field excited out of the focal plane, we can use a combination of Eq. 3.1 and 3.2 to model its propagation through the telescope and to the sky.

3.2 Review of the method

We developed an algorithm to calculate the angle-dependent response, or the beam, of a telescope using DIFFRACTIO [2], an open-source Python package, to model the propagation of light through free-space and diffracting apertures. DIFFRACTIO uses a time-reversed approach, where the detector is modeled as a light source whose emission propagates through the optical system to the image plane. To emulate the focal plane excitation, we leverage the diffractio.Scalar_Source_XY module, enabling the flexible generation of diverse source types with customizable spatial origins and angular propagation directions. Apertures

are modeled using the diffractio.Scalar_mask_XY module, which offers versatile creation of various mask shapes and types, allowing precise control over their amplitude, size, spatial placement, and tilt. For optical propagation, the diffractio.RS module is employed to compute the Rayleigh-Sommerfeld diffraction integral for near-field propagation, whereas the diffractio.FFT module handles far-field propagation via the Fraunhofer diffraction integral.

In this paper, we initiate our model not at the focal plane, but at the main-lobe defining entrance aperture of a telescope. Here, the Gaussian beam waist radius w(z) is determined by the f-number (N), wavelength (λ) , and the distance z to the focal plane. We have,

$$w(z) = w_0 \sqrt{1 + \left(\frac{z}{z_R}\right)^2} \tag{3.3}$$

where $z_R = \pi w_0^2/\lambda$ and $w_0 = 2\lambda N/\pi$. From the entrance aperture, the beam is allowed to propagate at specific angles to model the different pixels of the focal plane with defined wavelength. For subsequent apertures, we employ Rayleigh-Sommerfeld propagation to model the near-field intricacies of the resulting optical field. Figure 2 illustrates the near-field intensity for both edge and center pixels. After the final aperture, the light is allowed to propagate to the far-field. Prior to assessing the image in this region, a phase correction C is applied to the field, rendering the image plane orthogonal to the propagation wave-vector, following

$$C = e^{-i(k_x x + k_y y)}, (3.4)$$

where $k_x = k \sin \theta \cos \phi$, $k_y = k \sin \theta \sin \phi$ for k propagating along polar angle (θ, ϕ) .

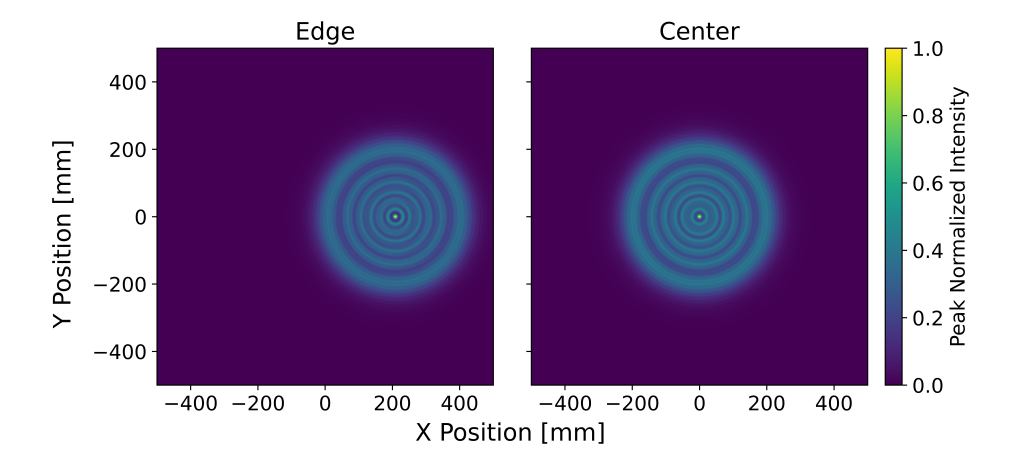


Figure 2. Peak normalized beam intensity at the sky-side of the baffle for edge (Left) and center (Right) pixels at 96 GHz.

4 Results

4.1 Simulated sidelobe maps

To demonstrate the accuracy of this method, we model the beam of the BICEP3 instrument and compare against the published beam profile in Giannakopoulos et al [3]. Given BICEP3's optical design, which steers the beam from a pixel on the focal plane to the center of the entrance aperture, we model its beam as originating from this aperture's center. In this

model, each distinct angle of propagation from the aperture's center emulates a different pixel on the focal plane, encompassing a uniform distribution of solid angles within the telescope's defined field of view (FOV) and incorporating the appropriate beam waist. Figure 2 shows the beam intensity at the entrance of the BICEP3 forebaffle for a center and edge pixel after computing the Rayleigh-Sommerfield diffraction integral of the fields at the entrance aperture. We multiply these near-field beams by the aperture function of the baffle and then compute their far-field diffraction integral to calculate the beam profile of a pixel of BICEP3. Figure 3 illustrates this beam profile on a HEALPix¹ [4] map for a center pixel, directed towards (latitude, longitude) = $(70^{\circ}, 110^{\circ})$. The BICEP3 optical parameters used in this study are listed in Table 1.

Table 1. Optical parameters of BICEP3 [5]

Optical parameters			
\overline{N}	1.6		
Observing band	[82.7, 109.5] GHz		
FOV diameter	27.4°		
F	$1078.32~\mathrm{mm}$		
D_0	$520~\mathrm{mm}$		
H_1	$1270~\mathrm{mm}$		
D_1	$1300~\mathrm{mm}$		

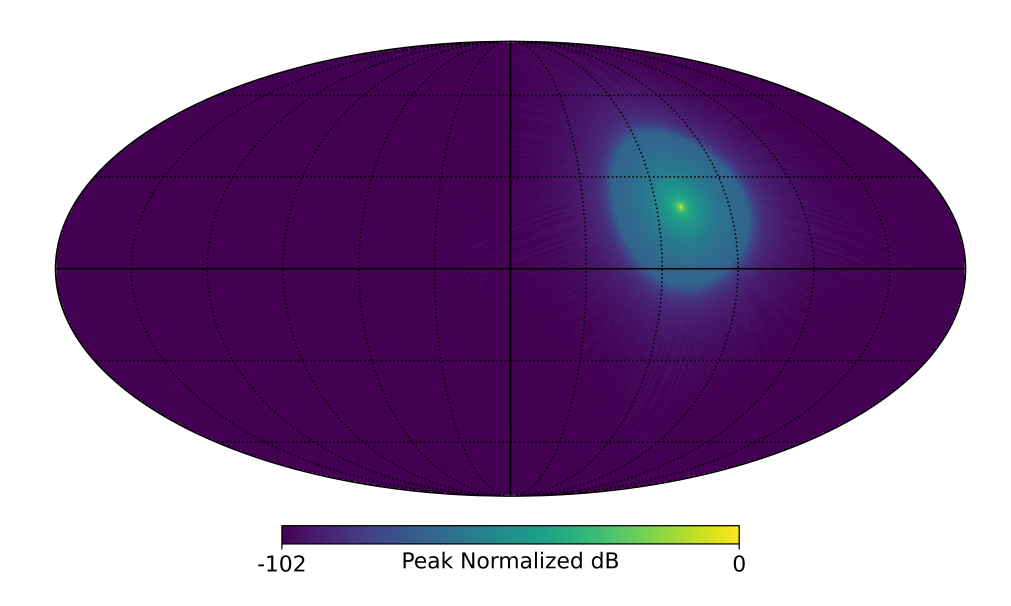


Figure 3. Peak normalized beam intensity in the far-field center (Right) pixels at 96 GHz, projected onto (latitude, longitude) = $(70^{\circ}, -110^{\circ})$.

The resulting beam profiles are presented in Figure 4 and 5. Figure 4 shows the bandand azimuthally-averaged beam profile for the center pixel, the edge pixel, and the profile averaged over the focal-plane, with and without the forebaffle. As expected, the forebaffle provides strong suppression of sidelobe power of more than 20 dB. Notably, the center pixel

https://healpix.sourceforge.io/

profile with the forebaffle exhibits a sharp power cutoff at approximately 33° , which corresponds to the geometric angle subtended between the far edges of the pupil aperture and the forebaffle.

As shown in Figure 5, the simulated beam profiles are in good agreement with the measured BICEP3 data from [3] across the main lobe and in macro-features like the primary cutoff angle. However, a noticeable deviation is observed in the far-angle sidelobe profile. This discrepancy is attributed to the fact that actual sidelobe power is not solely a product of diffraction but also incorporates contributions from other sources of stray light, such as scattering on the surfaces of various optical elements.

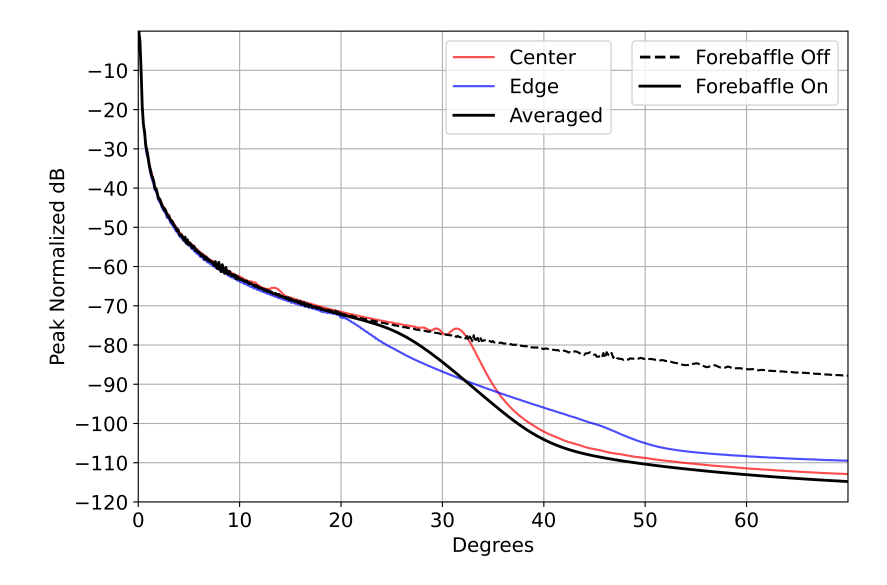


Figure 4. Band- and azimuthally-averaged beam profile of a BICEP3-like telescope, showing focal-plane averaged (black) beam, center (red) pixel beam, and edge (blue) pixel beam.

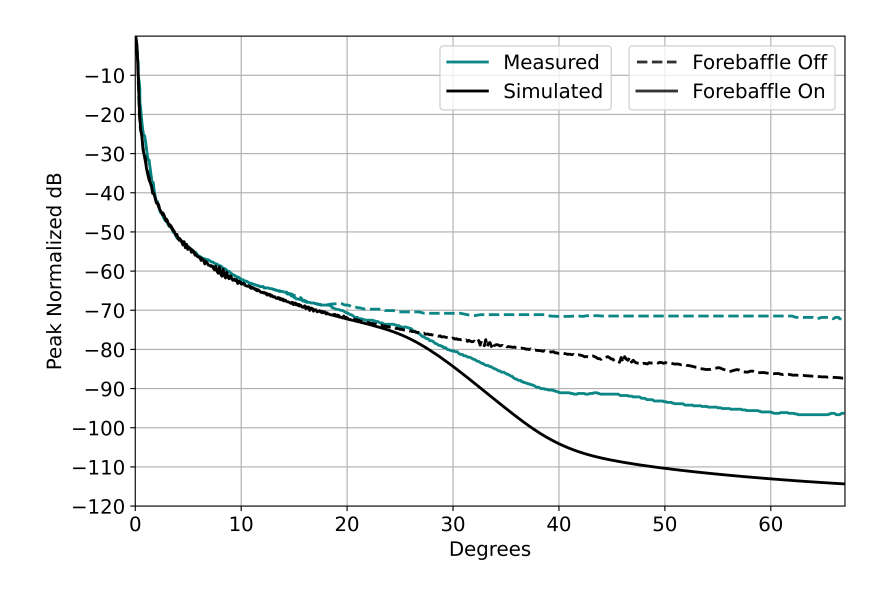


Figure 5. Band- and azimuthally-averaged beam profile of a BICEP3-like telescope, showing focal-plane averaged beam from simulations (black) and measurements by Giannakopoulos *et al* (teal).

4.2 Application to assess sidelobe pickup in Atacama Desert

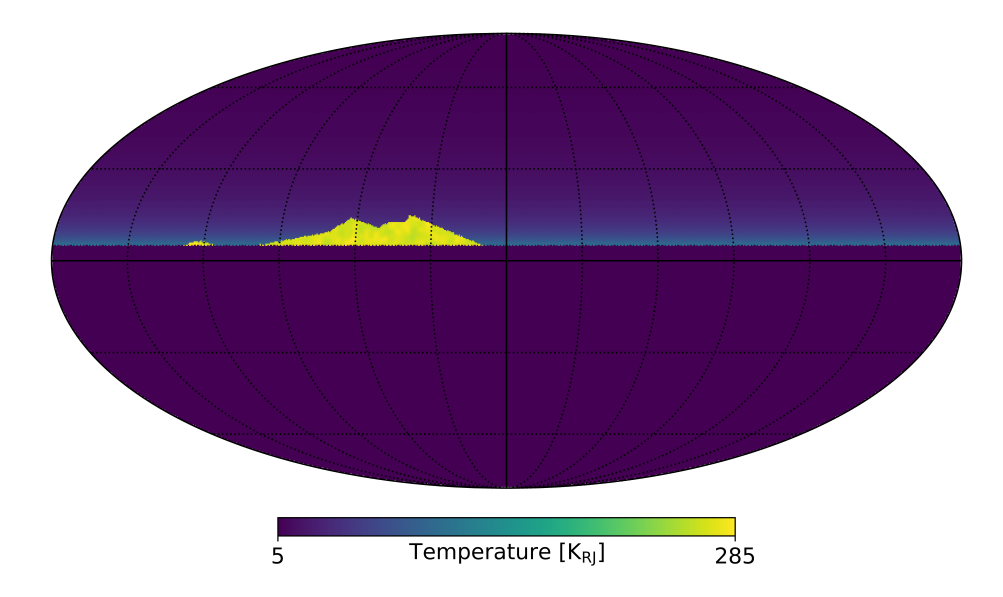


Figure 6. Temperature map of the environment containing emission from the sky, Cerro Toco, and ground shield.

We calculate the total sidelobe power pickup in the Rayleigh-Jean limit for a BICEP3-like telescope observing near the slopes of Cerro Toco in the Atacama Desert, where small aperture telescopes of Simons Observatory [6] are located. The simulation convolves the telescope's center detector beam with a HEALpix environment map, shown in Figure 6, incorporating emission from the sky, ground screen, and Cerro Toco. The sky temperature is modeled at 1 mm precipitable water vapor, with the atmospheric path length scaling with the cosecant of the observing elevation angle, as detailed in Errard et al. [7]. The ground screen extends up to 5° elevation and is assumed to perfectly reflect light from the telescope vertically, setting its temperature to that of the sky at zenith. The surface of Cerro Toco is modeled at 270 K temperature with fluctuations of 2° scale and 5 K RMS. The total sidelobe power pickup is determined by convolving this environment map with the beam map placed at a specific scanning coordinate (see Figure 3) and subtracting the azimuthally symmetric power pickup in the absence of Cerro Toco.

Figure 7 demonstrates the gain in sidelobe power pickup achieved using the forebaffle for scans at a constant elevation of 50° and 65° . The forebaffle provides substantial suppression of total power pickup at all azimuthal angles. With the telescope observing directly above Cerro Toco (azimuth of $\simeq 50^{\circ}$), the telescope sees over an order of magnitude more sidelobe power with the forebaffle off.

5 Conclusion

Next-generation CMB experiments and other centimeter to sub-millimeter experiments observing from the ground require exquisite control of systematic stray radiation pickup via instrumental far-sidelobe response. To meet this need, we have developed a diffraction-based beam modeling method that is simple and fast to directly inform the conceptual design of ground-based telescopes. When applied to model the BICEP3 far sidelobe radiation pattern,

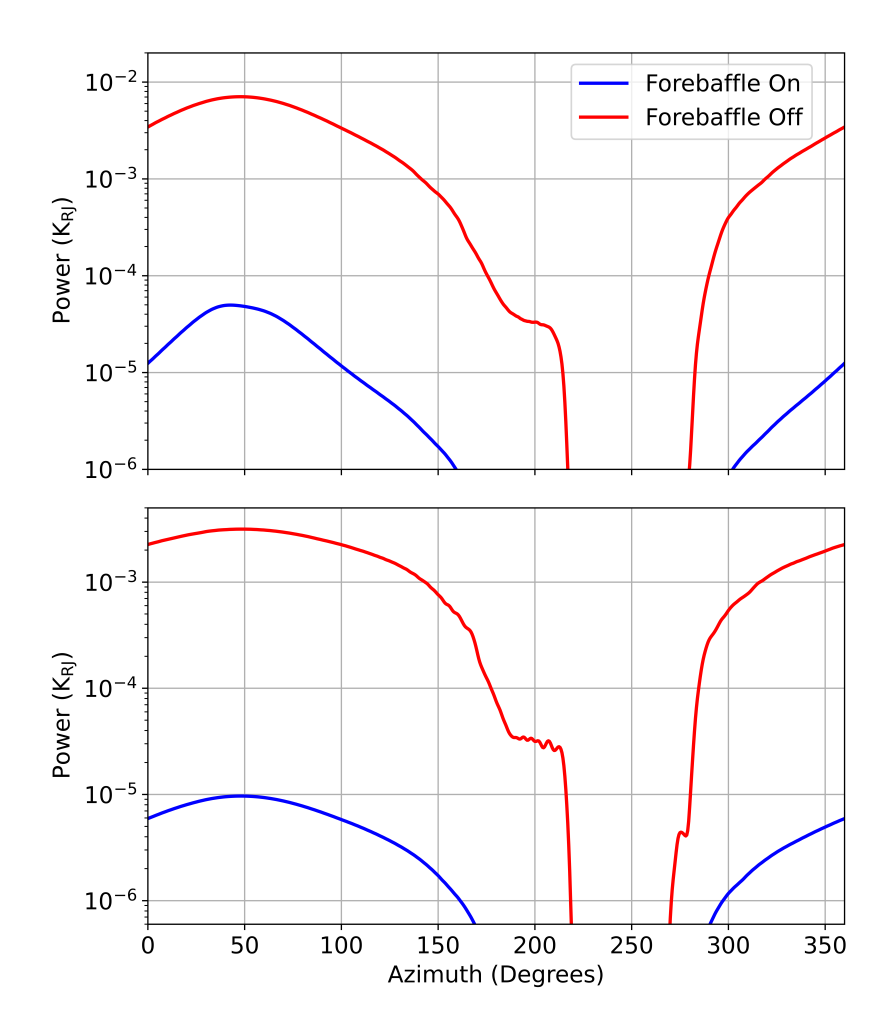


Figure 7. Power pickup from beam at 50° (top) and 65° (bottom) elevation scans.

our methodology shows good qualitative agreement with the *in situ* measured BICEP3 beam. This validated simulated beam was subsequently used to calculate the sidelobe pickup for a specific observation scenario near the slopes of Cerro Toco in the Atacama Desert. The simulation showed a significant difference in sidelobe pickup between the observation with the forebaffle on and the observation with the forebaffle off. This beam modeling method is most valuable as a tool for rapid comparison and optimization across various baffle geometries and instrument configurations, minimizing the need for highly detailed and computationally prohibitive full-wave simulations during the conceptual design phase.

Acknowledgments

The authors thank colleagues at LBNL—Bobby Besuner, Shamik Ghosh, John Groh, Reijo Keskitalo, Adrian T. Lee, and Clara Vergès, for useful discussions. Some of the results in this paper have been derived using the healpy and HEALPix packages.

References

- [1] J. Delabrouille, O. Jeong, M. Piat and A. Steier, "A novel double-rim forebaffle design for centimeter to sub-millimeter astrophysical observations." 2025.
- [2] L.M. Sanchez-Brea, A. Soria-Garcia, J. Andres-Porras, V. Pastor-Villarrubia, M.H. Elshorbagy, J. del Hoyo Muñoz et al., Diffractio: an open-source library for diffraction and interference calculations, in Optics and Photonics for Advanced Dimensional Metrology III, P.J. de Groot, F. Guzman and P. Picart, eds., vol. 12997, p. 129971B, International Society for Optics and Photonics, SPIE, 2024, DOI.
- [3] C. Giannakopoulos, C. Vergès, P.A.R. Ade, Z. Ahmed, M. Amiri, D. Barkats et al., Calibration measurements of the bicep3 and bicep array cmb polarimeters from 2017 to 2024, 2024.
- [4] K.M. Górski, E. Hivon, A.J. Banday, B.D. Wandelt, F.K. Hansen, M. Reinecke et al., Healpix: A framework for high-resolution discretization and fast analysis of data distributed on the sphere, Astrophys. J. 622 (2005) 759.
- [5] J.H. Kang, P.A.R. Ade, Z. Ahmed, R.W. Aikin, K.D. Alexander, D. Barkats et al., 2017 upgrade and performance of BICEP3: a 95GHz refracting telescope for degree-scale CMB polarization, in Millimeter, Submillimeter, and Far-Infrared Detectors and Instrumentation for Astronomy IX, J. Zmuidzinas and J.-R. Gao, eds., vol. 10708 of Society of Photo-Optical Instrumentation Engineers (SPIE) Conference Series, p. 107082N, July, 2018, DOI [1808.00567].
- [6] N. Galitzki, T. Tsan, J. Spisak, M. Randall, M. Silva-Feaver, J. Seibert et al., The Simons Observatory: Design, Integration, and Testing of the Small Aperture Telescopes, Astrophys. J. 274 (2024) 33 [2405.05550].
- [7] J. Errard, P.A.R. Ade, Y. Akiba, K. Arnold, M. Atlas, C. Baccigalupi et al., Modeling atmospheric emission for cmb ground-based observations, The Astrophysical Journal 809 (2015) 63.